HAL
open science

Synthesis and Spectral Properties of 6'-Triazolyl-Dihydroxanthene-Hemicyanine Fused Near-Infrared Dyes

Lingyue Gu, Kévin A Renault, Anthony Romieu, Jean-Alexandre Richard, Rajavel Srinivasan

To cite this version:

Lingyue Gu, Kévin A Renault, Anthony Romieu, Jean-Alexandre Richard, Rajavel Srinivasan. Synthesis and Spectral Properties of 6'-Triazolyl-Dihydroxanthene-Hemicyanine Fused Near-Infrared Dyes. New Journal of Chemistry, 2020, 44 (28), pp.12208-12215. 10.1039/D0NJ01724H . hal-03230412

HAL Id: hal-03230412

https://hal.science/hal-03230412v1

Submitted on 19 May 2021

HAL is a multi-disciplinary open access archive for the deposit and dissemination of scientific research documents, whether they are published or not. The documents may come from teaching and research institutions in France or abroad, or from public or private research centers.

L'archive ouverte pluridisciplinaire **HAL**, est destinée au dépôt et à la diffusion de documents scientifiques de niveau recherche, publiés ou non, émanant des établissements d'enseignement et de recherche français ou étrangers, des laboratoires publics ou privés.

Synthesis and Spectral Properties of 6'-Triazolyl-Dihydroxanthene-Hemicyanine Fused Near-Infrared Dyes

Lingyue Gu,[a] Kevin Renault,[b] Anthony Romieu,*[b] Jean-Alexandre Richard*[c] and Rajavel Srinivasan*[a]

We describe the synthesis of a range of 6'-triazolyl-dihydroxanthene-hemicyanine (DHX-hemicyanine) fused dyes through an effective copper-catalyzed azide-alkyne cycloaddition (CuAAC) "click" reaction, with the aim of providing molecular diversity and evaluating spectral properties of these near-infrared (NIR)-active materials. This was implemented by reacting 15 different aliphatic and aromatic azides with a terminal alkynyl-based-DHX-hemicyanine hybrid scaffold prepared in four steps and 35% overall yield from 4-bromosalicylaldehyde. The resulting triazole derivatives have been fully characterized and their optical properties determined both in organic solvents and simulated physiological conditions (phosphate buffered saline containing 5% of bovine serum albumin protein). This systematic study is a first important step towards the development of NIR-I fluorogenic "click-on" dyes or related photoactive agents for light-based diagnostic and/or therapeutic applications.

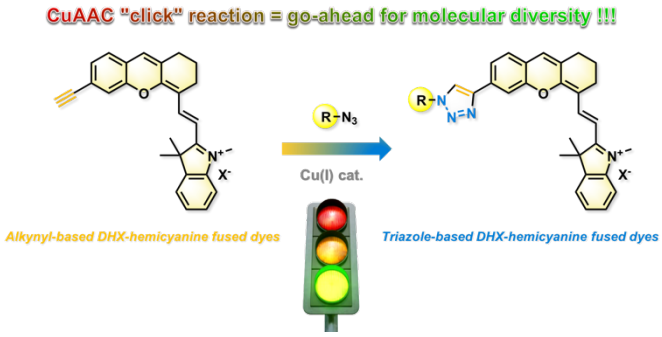

Introduction

The essence of "click chemistry" reactions lies in their simplicity, speed and robustness even in aqueous media.[1] While the concept has found popularity in organic chemistry, material science[2] and drug discovery,[3] it comes as no surprise that biologists have also embraced it to perform chemistry in living systems (known as *in vivo* chemistry).[4] By doing so, a new field coined bioorthogonal chemistry emerged and aims at developing advanced chemistry tools for the rational modification of biomolecules helping to a better understand of biology.[5] Of particular interest is the labelling of biomolecules monitoring their activity and leading to the discovery and/or deciphering of new biological mechanisms.

In this context, the association of reactions belonging to the repertoire of "click chemistry" with organic-based fluorophores has propulsed the field of bioorthogonal chemistry to an indispensable tool for the optical imaging of biological systems.[6] For instance, Meldal,[7] Sharpless and co-workers[8] rejuvenated the Huisgen 1,3-cycloaddition[9] and reported a regioselective Cu-catalyzed version (known as CuAAC for copper-catalyzed azide-alkyne cycloaddition) which has become the most iconic "click" reaction known so far.[10] Wang and co-workers applied it to fluorescent molecules and reported CuAAC reaction between 3-azidocoumarins and acetylenes.[11] While the aryl azide precursor did not display any fluorescence properties, the study showed that some of the triazoles formed turned fluorescent. In a similar fashion, Bertozzi's group used an azido aryl moiety as C9-substituent of xanthene-based fluorophores.[12] The initial azido rosamine did not emit any light because of a photoinduced electron transfer (PeT)-mediated quenching process. However, after evaluation of different positions of the azido group and electronic density of the aromatic ring, the fluorescence of the resulting triazole could be enhanced up to 58-fold (Scheme 1A).[13] Kele's group also used aryl azide precursors[14] but the approach using these scaffolds as fluorogenic precursors is limited because of their relative light instability and propensity to form the corresponding nitrene. It is possible to take advantage of this mechanism in the design of photoreactive cross-linkers suitable for photoaffinity labeling[15] but in the context of the development of fluorogenic probes that instability is a serious limitation.[16] One way around the need for an aryl azide precursor is to use a more stable terminal alkynyl-containing fluorophore. When the carbon-carbon triple bond replaces electron-donating groups (typically, *N*,*N*-dialkylamino moieties) it can turn the fluorophore to weakly or not fluorescent. This strategy was demonstrated by Tung's group on benzothiazoles[17] and by Yao and co-workers on

[a] G. Lingyue, Prof. R. Srinivasan
School of Pharmaceutical Science and Technology (SPST), Tianjin University, Building 24, 92 Weijin Road, Nankai District, Tianjin, 300072 P. R. China
E-mail: rajavels@tju.edu.cn
[b] Dr. K. Renault, Prof. A. Romieu
ICMUB, UMR 6302, CNRS, Univ. Bourgogne Franche-Comté
9, Avenue Alain Savary, 21000 Dijon, France
E-mail: anthony.romieu@u-bourgogne.fr
[c] Dr. J.-A. Richard
Functional Molecules and Polymers
Institute of Chemical and Engineering Sciences (ICES), Agency for Science, Technology and Research (A*STAR)
8 Biomedical Grove, Neuros, #07-01, Singapore 138665
E-mail: jean_alexandre@ices.a-star.edu.sg

†Electronic Supplementary Information (ESI) available: Protocols, NMR and HMRS data as well as copies of NMR spectra, HPLC traces and selected UV and fluorescence spectra.

rosamine- and xanthone-based fluorophores which displayed an increase of fluorescence emission upon formation of the triazole ring (Scheme 1B).[18]

Despite the advantages of longer-wavelength fluorescence light, known to facilitate molecular imaging in complex biological systems,[19] such strategies have mostly been implemented with fluorophores emitting in the visible spectral range and little progress has been made so far on the development of similar near-infrared (NIR)-emitting dyes (specifically, within NIR-I optical window 650-900 nm). Over the years, our respective groups have designed chemical methods leading to the development of a novel class of NIR-I dyes based on a molecular hybrid scaffold that combine both structural features of xanthene and cyanine parent compounds.[20] These dihydroxanthene (DHX)-hemicyanine fused fluorophores are now regarded as attractive alternatives to the popular and commonly used polymethine-cyanine dyes, as illustrated by numerous and valuable achievements in the fields of biosensing, bioimaging and theranostics.[21] Attracted by the modularity and ease of chemical modification of DHX-hemicyanine hybrid dyes, we set out to develop the access to a DHX precursor allowing the facile "click" formation of triazoles.

In a first attempt toward this goal, the introduction of an azido group on the 6'-position of the DHX skeleton proved to be a dead-end because of the marked photosensitivity of the aryl azide obtained. Instead, we took inspiration from our previous work to prepare an alkynyl-based DHX precursor **1** from the corresponding aryl bromide.[22] We then explored CuAAC reaction with aliphatic and aromatic azides. Finally, we determined the spectral properties of the resulting "clicked" fluorophores **2a-2o** to assess the influence of both triazole moiety and its substitution pattern on NIR absorption/emission ability of fused DHX-hemicyanine scaffold (Scheme 1B). Details of these investigations and their possible extensions are discussed in the present Article.

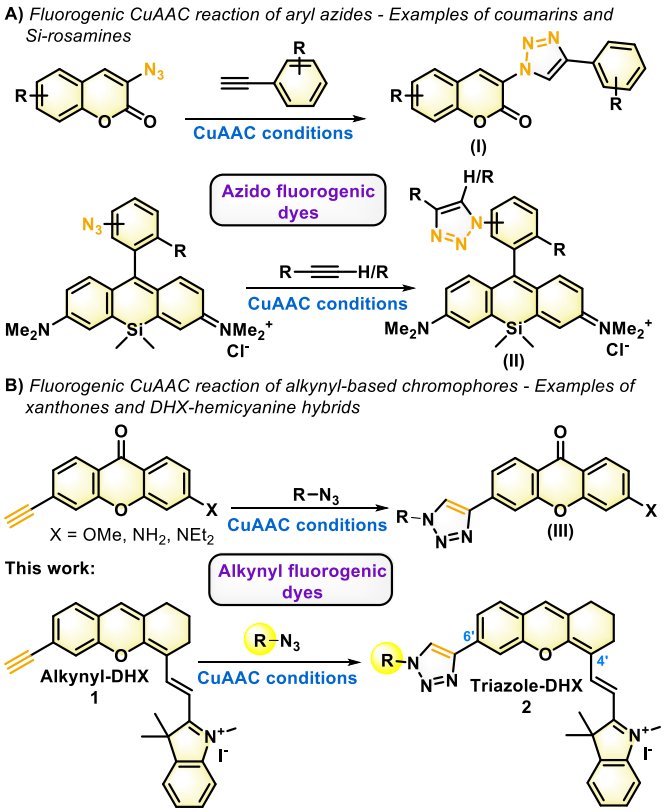

Scheme 1 CuAAC reaction for the development of fluorogenic "click-on" dyes. A) Reaction of 3-azidocoumarin and Si-rosamine fluorogenic dyes with terminal alkynes; B) Reaction of alkynyl-based xanthone and DHX fluorogenic dyes with azido compounds.

Results and discussion

Synthesis of a library of 6'-triazolyl-dihydroxanthene-hemicyanine fused dyes

We started our study with the preparation of the alkyne "click" partner **1** which we readily obtained in two steps from bifunctional arylbrominated aldehyde **6** (Scheme 2). This latter DHX-hemicyanine precursor was prepared in two steps from 3-bromophenol **3** through (1) Casnati-Skattebøl *ortho*-formylation ($MgCl_2$, $(HCHO)_n$, NEt_3)[23] that provided 4-bromosalicylaldehyde **4** in 69% yield, and its subsequent (2) one-pot reaction with enal **5** to form the DHX skeleton **6**. The aryl bromide moiety was then reacted with trimethylsilylacetylene **7** under Sonogashira reaction conditions ($Pd(PPh_3)_4$, CuI, 79% yield).[22] After removal of the TMS group under conventional conditions (K_2CO_3, CH_3OH), the formyl group was reacted with 1,2,3,3-tetramethyl-3*H*-indol-1-ium iodide (Fisher's base) **10** to yield the desired alkynyl-based DHX-hemicyanine fused dye **1** in 88% yield over two steps. The structure was proven by NMR and ESI mass analyses and the high level of purity (>94% whatever the wavelength used for the UV-vis detection) was confirmed by RP-HPLC-based analytical control (see ESI†).

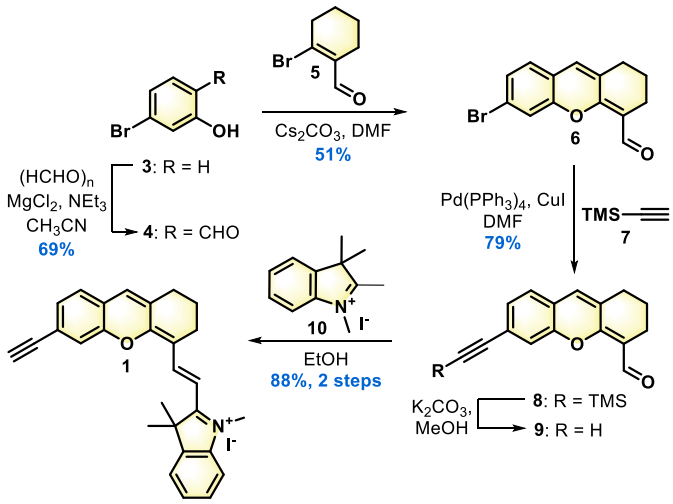

Scheme 2 Preparation of the alkynyl-based DHX-hemicyanine fused dye **1** in five steps from 3-bromophenol **3**.

We next explored reaction conditions allowing the formation of the desired triazole ring at the 6' position of the DHX-hemicyanine fused dye (Scheme 3A). To this end, we optimized the reaction conditions at room temperature in the presence of (3-azidopropyl)benzene **11a** as azido "click" partner, sodium ascorbate and various copper sources. While the use of copper(II) chloride and copper(II) sulfate pentahydrate provided some product (10% and 13% yield, respectively, Scheme 3A, entries 1-2), copper(II) acetate, copper(II) triflate and copper(I) chloride were much less successful (Scheme 3A, entries 3-6). Other usual "click" conditions using copper(I) sources without sodium ascorbate didn't provide any promising result either (Scheme 3A, entries 6 and 9). However, switching from the commonly used *tert*-butanol/water mixture of solvent to pure water in the presence of sodium ascorbate improved the yield significantly from 13% to 38% (Scheme 3A, entries 2 and 7). Ultimately, a mixture of DCM and water (Scheme 3A, entry 8) and 10 h reaction time appeared to be optimal (Scheme 3A, entries 10-12). With an interesting 50% yield (Scheme 3A, entry 8) it allowed us to explore the scope of the reaction with a wide range of alkyl and aryl azides **11b-o** (see ESI† for their synthesis).

A) *Screening of reaction conditions for CuAAC*

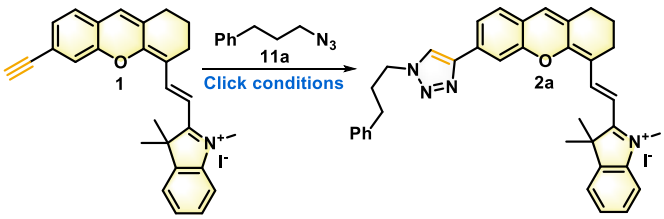

Entry	Solvent	Catalyst	Additive	Time (h)	Yield (%)[a]
1	DCM/H_2O (1:1)	$CuCl_2$	Na ascorbate	10	10
2	tBuOH/H_2O	$CuSO_4 \cdot 5H_2O$	Na ascorbate	10	13
3	THF	$Cu(OAc)_2$	Na ascorbate	10	0
4	THF	$Cu(OTf)_2$	Na ascorbate	10	Trace
5	EtOH	$Cu(OTf)_2$	Na ascorbate	10	Trace
6	CH_3CN	CuCl	NEt_3	10	0
7	H_2O	$CuSO_4 \cdot 5H_2O$	Na ascorbate	10	38
8	DCM/H_2O (1:1)	$CuSO_4 \cdot 5H_2O$	Na ascorbate	10	50
9	DCM/H_2O (1:1)	CuI	NEt_3	10	0
10	DCM/H_2O (1:1)	$CuSO_4 \cdot 5H_2O$	Na ascorbate	6	36
11	DCM/H_2O (1:1)	$CuSO_4 \cdot 5H_2O$	Na ascorbate	8	45
12	DCM/H_2O (1:1)	$CuSO_4 \cdot 5H_2O$	Na ascorbate	12	50

[a] Yield after purification by column chromatography over silica gel

B) *Scope of the synthesis of triazole-based DHX-hemicyanine hybrids*

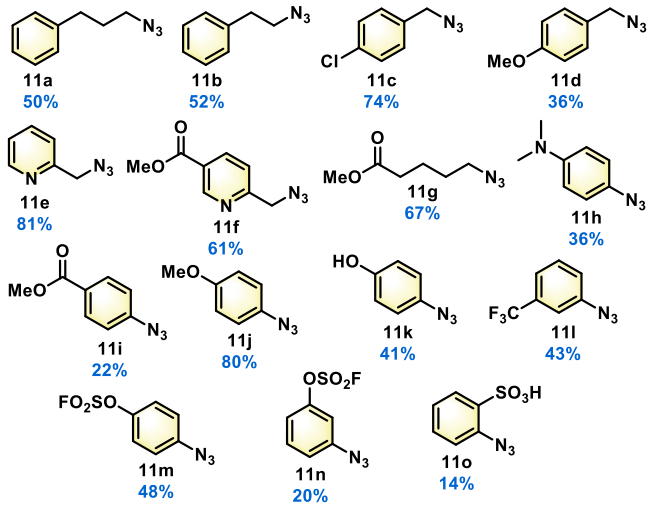

Scheme 3 A) Optimization of the CuAAC reaction for the synthesis of 6'-triazolyl-DHX-hemicyanine fused dyes **2**; B) Scope of the CuAAC reaction using aliphatic and aromatic azides.

With one less carbon in its alkyl chain, (2-azidoethyl)benzene **11b** behaved similarly to azide **11a** and formed the corresponding triazole **2b** in 52% yield. 4-Chloro- and 4-methoxybenzyl azide **11c** and **11d** were also successful (the corresponding triazoles **2c** and **2d** were isolated in 74% and 36% yields, respectively) and the two 2-(azidomethyl)pyridines **11e** and **11f** developed by the Ting group to speed-up the CuAAC reaction *in cellulo* gave triazole cycloadducts **2e** and **2f** in good 81% and 61% yields, respectively.[24] The availability of triazole-based fluorophores bearing an extra functional group for structural tuning or covalent conjugation to other (bio)molecular partners is of great interest for biological applications. The CuAAC reaction was therefore achieved with **11g**, **11i**, **11m** and **11n** to introduce either a latent carboxylic acid (masked as methyl ester) or an aryloxysulfonyl fluoride moiety (this latter one being identified as an effective reactive

partner in "click" reaction sulfur(VI) fluoride exchange (SuFEx)[25]). The possible influence of an electron-donating or -withdrawing substituent introduced on triazole moiety, over spectral properties of the resulting "clicked" DHX-based dyes, was also addressed through the successful synthesis of **2h-2l**. Finally, the presence of an *ortho*-substituted sulfonic acid group in **11o** provided a simple way to introduce a polar group facilitating the water-solubilization of the resulting DHX-hemicyanine fused dye **2o** (Scheme 3B). The structures of these 15 novel triazole-based DHX-hemicyanine fused dyes were unambiguously confirmed by ESI-HRMS and NMR spectroscopic analyses (see ESI†). Their purity was checked by RP-HPLC and found to be above 95%, value usually required to achieve relevant photophysical measurements.

Photophysical properties of 6'-triazolyl-dihydroxanthene-hemicyanine fused dyes

To assess changes in photophysical properties after triazole formation, we next studied the spectral behavior of our library of 15 DHX-hemicaynine fused dyes **2a-2o** and alkynyl precursor **1** in different media including phosphate buffered saline (PBS) with 5% (w/v) bovine serum albumin (BSA) as simulated body fluid, EtOH, and $CHCl_3$ (Table 1 and Fig. 1 for the Abs/Ex/Em spectra of **1** and **2o** in $CHCl_3$ and in PBS + 5% BSA, see ESI† for Abs/Ex/Em spectra of other compounds). A first general trend common to all triazole-based dyes and alkyne **1** is the dramatic broadening of the main absorption band assigned to S_0-S_1 electronic transition, compared to that of more conventional DHX-hemicyanine fused fluorophore bearing a *N*,*N*-dialkylamino group as C-6' substituent like **12**, which explains the notable lower molar extinction coefficient of dyes **2a**-**2o** compared to **12**. A full-width half maximum (FWHM), $\Delta\lambda_{1/2\ max}$ in the range of 3410-4370 cm^{-1} is observed depending primarily on the solvent used, against only 695-990 nm for **12** and unlike the latter, well-defined vibronic structures with two maxima and one pronounced blue-shifted shoulder are observed in all absorption spectra. The lack of an effective electron-donating group such as $-NEt_2$, on C-6' position, induces an expected hypsochromic shift of ca. 50 nm or 100 nm depending the local absorption maximum regarded for the triazole derivatives, of the maximum absorption peak position for the DHX-hemicyanine hybrid scaffold. This feature also contributes to the dramatic decrease of molar extinction coefficients compared to those of more conventional DHX-based fluorophores such as **12**.

Red excitation at 620 nm produced the desired NIR emission in the form of a vibronic structure with two well-defined maxima in the range 690-760 nm. However, only a very weak fluorescence emission intensity was observed, whatever the triazole derivative studied, the solvent and concentration range (1-10 μM) used. It prevented us to accurately determine relative fluorescence quantum yields, roughly

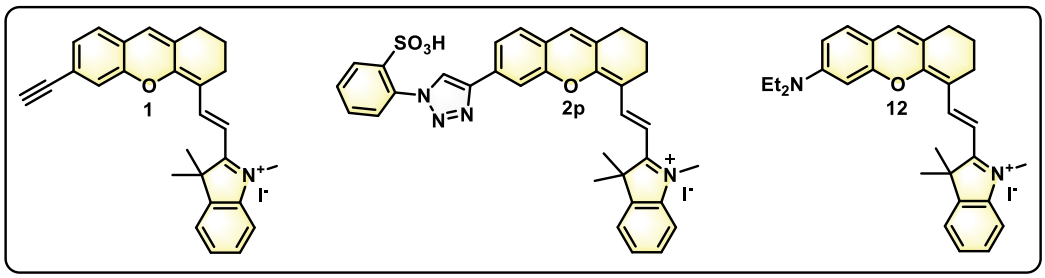

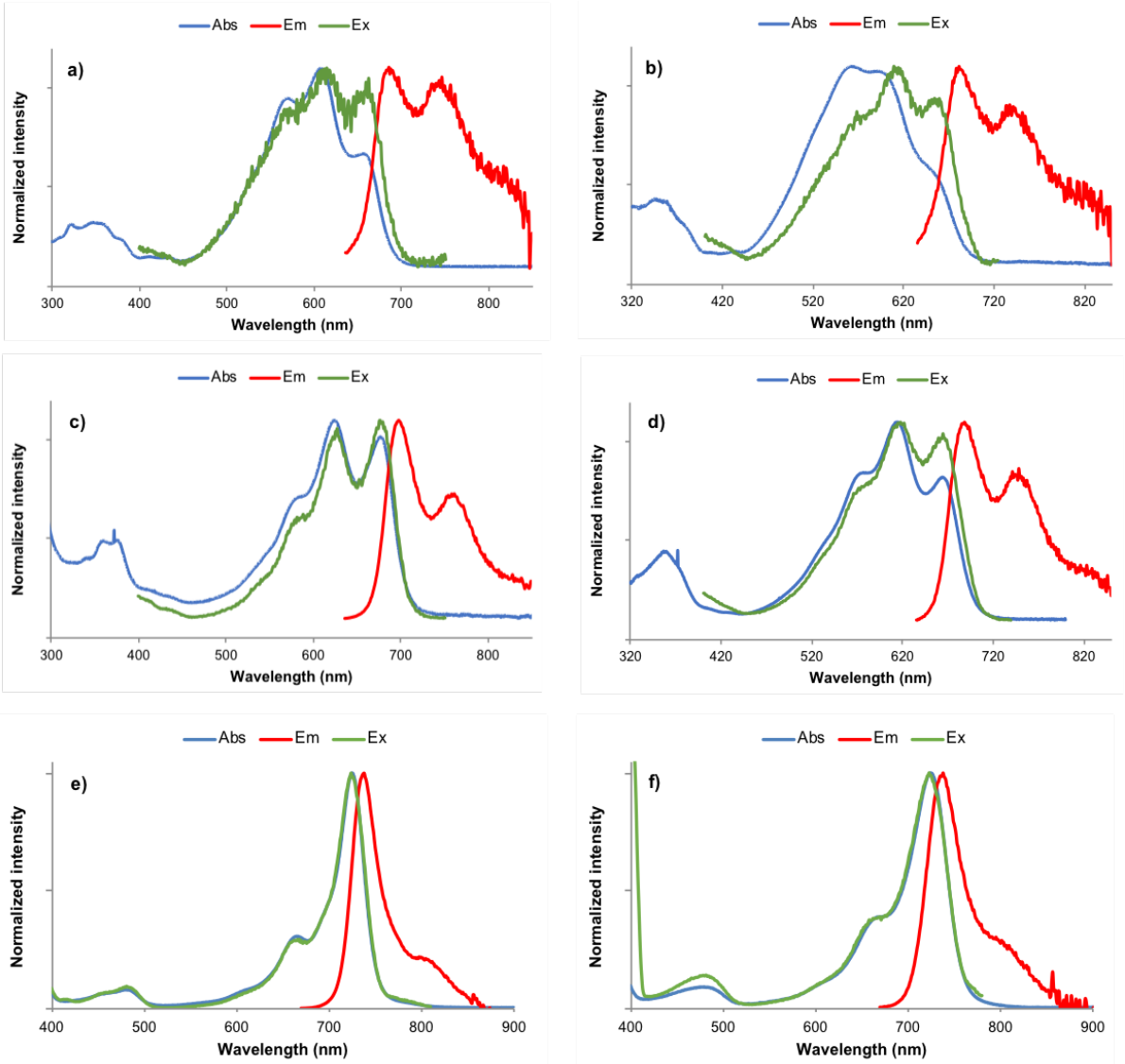

Fig. 1 Normalised absorption, emission (excitation at 620 nm for a-d and 650 nm for e-f) and excitation (emission at 760 nm for a-d, 830 nm for e or 800 nm for f) spectra of alkynyl-based DHX-hemicyanine fused dye **1** (a in $CHCl_3$ and b in PBS + 5% BSA), triazole-based DHX-hemicyanine fused dye **2o** (c in $CHCl_3$ and d in PBS + 5% BSA), and *N*,*N*-diethylamino-DHX-hemicyanine fused dye **12** (e in $CHCl_3$ and f in PBS + 5% BSA). For the excitation spectrum of **12** in PBS + 5% BSA, a peak at 400 nm ($\lambda_{ex}/2$) assigned to Rayleigh scattering is observed. See the Experimental section for details about these measurements.

estimated at less than 1%. The very low values of these quantum yields cannot be attributed to the formation of non-emissive aggregates (*i.e.*, H-type homodimers)[26] because a good matching between the absorption and excitation spectra was observed except for some triazole derivatives (*e.g.*, **2i**, **2l** and **2m**, see ESI†) and **1** spectrally characterised in simulated physiological conditions (*i.e.*, PBS + 5% BSA). The capability of BSA protein to disrupt fluorophore aggregates in aq. media is well-documented but in the present case, its surfactant behavior was not sufficiently effective to obtain a single emissive species in solution.[27] Alternatively, we attempted to assess the relative fluorescence efficiency of dyes **2a**-**2o** and **1** by calculating the ratio [(integration of emission curve)/absorption at 620 nm)] for

a single concentration (5 μM) solution in $CHCl_3$ of each compound (**1** and **2a-2o**). We observed a change in color of solution from sapphire blue (for alkyne **1**) to sky blue (for triazole derivatives **2a-2o**) (see ESI†) but could not obtain reliable values allowing an accurate and relevant ranking of the fluorophores synthesized in this study, based on their emissive capability.

Conclusions

Quest for high-performance NIR-I chromophores/fluorophores based on the attractive DHX-hemicyanine hybrid scaffold led us to consider for the first time CuAAC "click" reaction as a simple way of achieving high molecular diversity through the straightforward synthesis of alkynyl-based DHX-hemicyanine fused dye **1** and its "click" derivatisation with a wide range of organic azides. In contrast to already published fluorogenic alkynes photoactive in the blue-green spectral range, only a weak fluorescence emission of triazole-based dyes was observed within the NIR-I window. Thus, our efforts that involved synthesis and photophysical characterization of a library of 15 different compounds will require a further structural optimization to obtain NIR-I fluorogenic "click-on" dyes suitable for bioimaging. Interestingly, the specific molecular absorption signature of both alkyne and triazole derivatives (*i.e.*, broad, structured and weakly solvent dependent absorption band) might be used to design novel broad spectrum dark quencher molecules suitable for the construction of far-red or NIR-I fluorescence light-up probes based on Förster resonance energy transfer (FRET) mechanism.[28]

Experimental†

See ESI† for the details about sections "General", "Instruments and methods", and all experimental and spectral data associated with synthesised compounds.

Synthesis

6-((Trimethylsilyl)ethynyl)-2,3-dihydro-1*H*-xanthene-4 carbaldehyde (8). $Pd(PPh_3)_4$ (67.5 mg, 8.3 mmol%) and CuI (23.6 mg, 0.1 mmol) were degassed in a flame-dried round bottom flask. NEt_3 (1.2 mL, 8.3 mmol) in dry DMF (10 mL) was added with aryl bromide **6** (1.2 g, 4.1 mmol). The solution was degassed again then trimethylsilylacetylene **7** was added (1.8 mL, 12.4 mmol). The reaction mixture was heated to 85 °C for 24 h. After being cooled to room temperature, the reaction mixture was concentrated under vacuum and the resulting residue was purified by flash-column chromatography on silica gel (eluent: 1% EtOAc in PE) affording pure TMS-protected terminal alkyne **8** as a orange solid (1.0 g, yield 79%). ^{1}H NMR (400 MHz, $CDCl_3$): δ = 10.30 (s, 1 H), 7.17 (s, 1 H), 7.13 (dd, *J* = 7.8 Hz, *J* = 1.2 Hz, 1 H), 7.05 (d, *J* = 7.8 Hz, 1 H), 6.62 (s, 1 H), 2.58 (ddd, *J* = 7.5 Hz, *J* = 5.8 Hz, *J* = 1.6 Hz, 2 H), 2.43 (t, *J* = 6.0 Hz, 2 H), 1.71 (m, 2 H), 0.25 (s, 9 H); ^{13}C NMR (101 MHz, $CDCl_3$): δ = 188.0, 159.9, 151.7, 130.8, 127.6, 126.5, 126.1, 124.6, 121.6, 118.6, 113.8, 104.0, 96.9, 30.3, 21.6, 20.4, 0.0 ppm; HRMS (ESI+): *m/z* 331.1141 [M + Na]$^+$, calcd for $C_{19}H_{20}O_2SiNa^+$ 331.1125.

6-Ethynyl-2,3-dihydro-1*H*-xanthene-4-carbaldehyde (9). TMS-protected terminal alkyne **8** (1.0 g, 3.3 mmol) was dissolved in dry MeOH (30 mL) and treated with anhydrous K_2CO_3 (1.8 g, 13.2 mmol). The mixture was stirred at room temperature for 5 h. The solvent was removed, and the residue was taken up in 100 mL of DCM and washed with 100 mL of deionised water. The organic layer was dried over anhydrous Na_2SO_4 and concentrated under reduced pressure. This compound was used in the next step without further purification, and the yield was assumed to be quantitative. ^{1}H NMR (400 MHz, DMSO-d_6): δ = 10.26 (s, 1 H), 7.36 (d, *J* = 7.9 Hz, 1 H), 7.34 (s, 1 H), 7.24 (dd, *J* = 7.8 Hz, *J* = 1.5 Hz, 1 H), 7.01 (s, 1 H), 4.37 (s, 1 H), 2.59 (ddd, *J* = 7.0 Hz, *J* = 5.3 Hz, *J* = 1.6 Hz, 2 H), 2.30 (t, *J* = 6.0 Hz, 2 H), 1.63 (m, 2 H) ppm; ^{13}C NMR (101 MHz, $CDCl_3$): δ = 188.1, 159.8, 151.7, 131.1, 127.7, 126.6, 125.9, 123.6, 122.0, 118.9, 113.9, 82.8, 79.3, 30.3, 21.6, 20.4 ppm; HRMS (ESI+): *m/z* 237.0910 [M + H]$^+$, calcd for $C_{16}H_{13}O_2^+$ 237.0910.

Alkynyl-based DHX-hemicyanine fused dye (1). To aldehyde **9** (236 mg, 1.0 mmol) in EtOH (2 mL) was added 1,2,3,3-tetramethyl-3*H*-indol-1-ium iodide **10** (301 mg, 1.0 mmol) and the solution was refluxed at 80 °C for 4 h. The reaction mixture was concentrated and the crude product was purified by flash-column chromatography on silica gel (eluent: 1% MeOH in DCM) to afford alkynyl-DHX **1** as a dark blue solid (345 mg, yield 88%). m.p >300 °C; ^{1}H NMR (400 MHz, DMSO-d_6): δ = 8.56 (d, *J* = 15.3 Hz, 1 H), 7.80-7.73 (m, 2 H), 7.62 (s, 1 H), 7.58 (m, 1 H), 7.52 (m, 2 H), 7.39-7.33 (m, 2 H), 6.68 (d, *J* = 15.4 Hz, 1 H), 4.52 (s, 1 H), 3.95 (s, 3 H), 2.72 (t, *J* = 6.0 Hz, 2 H), 2.67 (t, *J* = 6.0 Hz, 2 H), 1.83 (m, 2 H), 1.77 (s, 6 H) ppm; ^{13}C NMR (101 MHz, DMSO-d_6): δ = 179.0, 158.0, 151.8, 145.1, 142.4, 142.1, 131.1, 129.8, 128.8, 128.4, 127.8, 127.6, 123.8, 122.6, 122.2, 118.6, 114.3, 113.8, 107.2, 83.8, 82.6, 50.8, 33.2, 28.7, 26.9, 23.5, 19.7 ppm; HRMS (ESI+): *m/z* 392.2019 [M]$^{+\bullet}$, calcd for $C_{28}H_{26}NO^+$ 392.2009; HPLC (system A): t_R = 4.9 min (purity 94% at 260 nm and 98% at 600 nm); LRMS (ESI+, recorded during RP-HPLC analysis): *m/z* 392.3 [M]$^{+\bullet}$ (100), calcd for $C_{28}H_{26}NO^+$ 392.2; UV-vis (recorded during the HPLC analysis): λ_{max} = 559 and 592 nm (broad band).

General procedure for the synthesis of tetrazole-based DHX-hemicyanine fused dyes 2a-2o. To a mixture of alkynyl-based DHX-hemicyanine dye **1** (784 mg, 2.0 mmol, 1.0 equiv.) and the corresponding organic azide **11a-o** (2.6 mmol, 1.3 equiv.) in deionised water and CH_2Cl_2 (1:1 (v/v), 100 mL), sodium ascorbate (79.2 mg, 0.4 mmol, 0.2 equiv.) was added, followed by the addition of $CuSO_4 \bullet 5\ H_2O$ (25 mg, 0.1 mmol, 0.05 equiv.). The heterogeneous mixture was stirred vigorously at room temperature overnight. Thereafter, the reaction mixture was concentrated under reduced pressure and directly purified by flash-column chromatography on silica gel (eluent: 1% MeOH in DCM) to afford the corresponding triazole **2a-2o** as a dark blue amorphous powder.

Photophysical characterisations

UV-visible spectra were obtained either on a Varian Cary 50 scan (single-beam) or an Agilent technologies 60 (single-beam) spectrophotometer (software Cary WinUV) by using rectangular quartz cells (Hellma, 100-QS, 45 × 12.5 × 12.5 mm, pathlength: 10 mm, chamber volume: 3.5 mL), at 25 °C (using a temperature control system combined with water circulation). Fluorescence spectra (emission/excitation spectra) were recorded with an HORIBA Jobin Yvon Fluorolog spectrofluorometer (FluorEssence software) at 25 °C (using a temperature control system combined with water circulation), with standard fluorometer

cells (Labbox, LB Q, light path: 10 mm, width: 10 mm, chamber volume: 3.5 mL). The absorption and fluorescence emission spectra were recorded with dye solutions of concentrations in the range of 10^{-5}-10^{-6} M. The emission spectra were recorded in the range of 635-850 nm after excitation at 620 nm (shutter: Auto Open, integration time = 0.1 s, 1 nm step, HV(S1) = 950 V, excitation slit = 5 nm and emission slit = 5 nm). The excitation spectra were recorded in the range of 400-750 nm after emission at 760 nm (excitation slit = 5 nm for spectra recorded in $CHCl_3$ and 12 nm for spectra recorded in EtOH or PBS + 5% BSA and emission slit = 5 nm). All excitation/emission spectra are corrected.

Conflicts of interest

The authors declare no conflict of interest.

Acknowledgements

This work is supported by SPST, Tianjin University (P.R. China), ICES, A*STAR (Singapore), and the CNRS, Université de Bourgogne and Conseil Régional de Bourgogne through the "Plan d'Actions Régional pour l'Innovation (PARI) and the "Fonds Européen de Développement Régional (FEDER)" programs. Financial supports from Agence Nationale de la Recherche (ANR, AAPG 2018, PRCI LuminoManufacOligo, ANR-18-CE07-0045-01), especially for the post-doc fellowship of K. R., the National Research Foundation Singapore (NRF, LuminoManufacOligo, NRF2018-NRF-ANR035) and GDR CNRS "Agents d'Imagerie Moléculaire" (AIM) 2037 are also greatly acknowledged. The authors thank Ms Doris Tan (ICES, Singapore) and Dr. Quentin Bonnin (CNRS, PACSMUB) for the recording of HRMS spectra. A. R. and K. R thank the "Plateforme d'Analyse Chimique et de Synthèse Moléculaire de l'Université de Bourgogne" (PACSMUB, http://www.wpcm.fr) for access to spectroscopy instrumentation.

Notes and references

1 H. C. Kolb, M. G. Finn and K. B. Sharpless, *Angew. Chem. Int. Ed.*, 2001, **40**, 2004.
2 (a) J.-F. Lutz, *Angew. Chem. Int. Ed.*, 2007, **46**, 1018; (b) H. Nandivada, X. Jiang and J. Lahann, *Adv. Mater.*, 2007, **19**, 2197.
3 H. C. Kolb and K. B. Sharpless, *Drug Discov. Today*, 2003, **8**, 1128.
4 (a) J. A. Prescher and C. R. Bertozzi, *Nat. Chem. Biol.*, 2005, **1**, 13; (b) M. Boyce and C. R. Bertozzi, *Nat. Methods*, 2011, **8**, 638; (c) C. R. Bertozzi and P. Wu, *Curr. Opin. Chem. Biol.*, 2013, **17**, 717; (d) J. G. Rebelein and T. R. Ward, *Curr. Opin. Biotechnol.*, 2018, **53**, 106.
5 (a) J. M. Baskin and C. R. Bertozzi, *QSAR & Comb. Sci.*, 2007, **26**, 1211; (b) E. M. Sletten and C. R. Bertozzi, *Angew. Chem. Int. Ed.*, 2009, **48**, 6974; (c) E. M. Sletten and C. R. Bertozzi, *Acc. Chem. Res.*, 2011, **44**, 666.
6 (a) C. Le Droumaguet, C. Wang and Q. Wang, *Chem. Soc. Rev.*, 2010, **39**, 1233; (b) P. Shieh and C. R. Bertozzi, *Org. Biomol. Chem.*, 2014, **12**, 9307.
7 (a) C. W. Tornøe, C. Christensen and M. Meldal, *J. Org. Chem.*, 2002, **67**, 3057; (b) M. Meldal and C. W. Tornøe, *Chem. Rev.*, 2008, **108**, 2952.
8 V. V. Rostovtsev, L. G. Green, V. V. Fokin and K. B. Sharpless, *Angew. Chem. Int. Ed.*, 2002, **41**, 2596.
9 R. Huisgen, *Proc. Chem. Soc.*, 1961, 357.
10 D. Brunel and F. Dumur, *New J. Chem.*, 2020, **44**, 3546.
11 K. Sivakumar, F. Xie, B. M. Cash, S. Long, H. N. Barnhill and Q. Wang, *Org. Lett.*, 2004, **6**, 4603.
12 (a) P. Shieh, M. J. Hangauer and C. R. Bertozzi, *J. Am. Chem. Soc.*, 2012, **134**, 17428; (b) P. Shieh, V. T. Dien, B. J. Beahm, J. M. Castellano, T. Wyss-Coray and C. R. Bertozzi, *J. Am. Chem. Soc.*, 2015, **137**, 7145.
13 P. Shieh, M. S. Siegrist, A. J. Cullen and C. R. Bertozzi, *Proc. Natl. Acad. Sci. U S A*, 2014, **111**, 5456.
14 (a) A. Herner, I. Nikić, M. Kállay, E. A. Lemke and P. Kele, *Org. Biomol. Chem.*, 2013, **11**, 3297; (b) G. B. Cserép, A. Herner and P. Kele, *Methods Appl. Fluoresc.* , 2015, **3**, 042001; (c) Z. Pünkösti, P. Kele and A. Herner, *J. Het. Chem.*, 2018, **55**, 1183.
15 G. T. Hermanson, in *Bioconjugate Techniques (Third Edition)*, Academic Press, Boston, 2013, ch. 3, pp. 253.
16 E. Păunescu, L. Louise, L. Jean, A. Romieu and P.-Y. Renard, *Dyes Pigm.*, 2011, **91**, 427.
17 (a) J. Qi and C.-H. Tung, *Bioorg. Med. Chem. Lett.*, 2011, **21**, 320; (b) J. Qi, M.-S. Han, Y.-C. Chang and C.-H. Tung, *Bioconjugate Chem.*, 2011, **22**, 1758.
18 J. Li, M. Hu and S. Q. Yao, *Org. Lett.*, 2009, **11**, 3008.
19 (a) R. Weissleder and U. Mahmood, *Radiology*, 2001, **219**, 316; (b) J. V. Frangioni, *Curr. Opin. Chem. Biol.*, 2003, **7**, 626; (c) I. Martinić, S. V. Eliseeva and S. Petoud, *J. Lumin.*, 2017, **189**, 19.
20 (a) J.-A. Richard, *Org. Biomol. Chem.*, 2015, **13**, 8169; (b) A. Romieu and J.-A. Richard, *Tetrahedron Lett.*, 2016, **57**, 317; (c) M. J. H. Ong, S. Debieu, M. Moreau, A. Romieu and J.-A. Richard, *Chem. Asian J.*, 2017, **12**, 936; (d) S. Zheng, G. Lingyue, M. J. H. Ong, D. Jacquemin, A. Romieu, J.-A. Richard and R. Srinivasan, *Org. Biomol. Chem.*, 2019, **17**, 4291.
21 H. Chen, B. Dong, Y. Tang and W. Lin, *Acc. Chem. Res.*, 2017, **50**, 1410.
22 M. J. H. Ong, R. Srinivasan, A. Romieu and J.-A. Richard, *Org. Lett.*, 2016, **18**, 5122.
23 (a) N. U. Hofsløkken and L. Skattebøl, *Acta Chem. Scand.*, 1999, **53**, 258; (b) T. V. Hansen and L. Skattebøl, *Org. Synth.*, 2005, **82**, 64; (c) T. V. Hansen and L. Skattebøl, *Org. Synth.*, 2012, **89**, 220.
24 C. Uttamapinant, A. Tangpeerachaikul, S. Grecian, S. Clarke, U. Singh, P. Slade, K. R. Gee and A. Y. Ting, *Angew. Chem. Int. Ed.*, 2012, **51**, 5852.
25 (a) J. Dong, L. Krasnova, M. G. Finn and K. B. Sharpless, *Angew. Chem. Int. Ed.*, 2014, **53**, 9430; (b) A. S. Barrow, C. J. Smedley, Q. Zheng, S. Li, J. Dong and J. E. Moses, *Chem. Soc. Rev.*, 2019, **48**, 4731; (c) A. Marra, C. Nativi and A. Dondoni, *New J. Chem.*, 2020, **44**, 4678.
26 M. Ogawa, N. Kosaka, P. L. Choyke and H. Kobayashi, *ACS Chem. Biol.*, 2009, **4**, 535.
27 Pauli, M. Grabolle, R. Brehm, M. Spieles, F. M. Hamann, M. Wenzel, I. Hilger and U. Resch-Genger, *Bioconjugate Chem.*, 2011, **22**, 1298.
28 (a) T. Myochin, K. Hanaoka, S. Iwaki, T. Ueno, T. Komatsu, T. Terai, T. Nagano and Y. Urano, *J. Am. Chem. Soc.*, 2015, **137**, 4759; (b) J. Demuth, R. Kucera, K. Kopecky, Z. Havlínová, A. Libra, V. Novakova, M. Miletin and P. Zimcik, *Chem. Eur. J.*, 2018, **24**, 9658.
.

Table 1 Photophysical properties of alkynyl-based DHX-hemicyanine fused dye **1**, triazole derivatives **2a-2o** and reference dye **12**[22] at 25 °C. For structures, see ESI†.

Entry	Dye	Abs max[a] [nm]			Em max[c,d] [nm]			ε [M^{-1} cm^{-1}]			Stokes' shift[e] [cm^{-1}]		
		$CHCl_3$	EtOH	PBS[b]	$CHCl_3$	EtOH	PBS	$CHCl_3$	EtOH	PBS	$CHCl_3$	EtOH	PBS
1	**1**	569 607 654	562 597 640	566 598 645	685 746	675 728	681 741	25 700 45 200 38 300	38 750 42 200 22 850	31 150 31 000 16 700	1876	1935	2038
2	**2a**	579 617 670	572 608 656	578 614 662	693 755	686 741	688 751	34 200 52 050 40 600	35 200 44 200 28 200	28 600 34 550 22 500	1777	1870	1752
3	**2b**	579 619 671	573 608 656	575 612 661	691 755	685 742	687 748	41 800 63 500 48 600	42 100 53 100 33 700	35 700 41 250 26 450	1683	1849	1784
4	**2c**	579 618 670	571 607 656	573 612 662	692 752	684 744	688 747	38 100 58 900 45 800	45 100 56 450 35 500	36 700 39 300 25 300	1730	1854	1805
5	**2d**	579 618 670	571 608 656	573 611 663	693 754	685 749	686 748	40 400 59 050 43 500	44 250 55 850 35 600	38 500 41 000 27 050	1751	1849	1789
6	**2e**	580 620 671	572 607 656	570 607 661	694 751	685 745	688 741	42 100 62 200 46 100	43 050 54 150 34 200	38 950 35 700 23 350	1720	1876	1939
7	**2f**	580 618 669	571 607 656	576 613 662	694 758	687 743	686 749	37 200 55 300 41 500	35 750 44 800 28 250	30 500 38 700 27 500	1772	1918	1736
8	**2g**	580 620 672	571 607 657	572 610 661	694 758	686 746	686 751	37 800 58 400 45 500	39 350 49 600 31 400	33 700 35 700 23 750	1720	1897	1816
9	**2h**	583 621 672	574 609 658	583 616 667	693 755	684 746	688 751	23 250 37 400 30 900	27 000 33 700 21 450	22 800 25 950 17 100	1673	1800	1700
10	**2i**	581	572	570	695	685	689	37 800	41 500	33 100	1766	1849	2015

		619 670	608 656	605 674	758	748	751	56 700 43 700	51 150 31 650	25 650 14 100			
11	**2j**	580 620 671	572 608 657	577 612 667	697 758	687 749	691 746	38 700 58 600 45 350	44 700 56 000 35 350	35 300 38 700 25 800	1782	1891	1868
12	**2k**	581 619 671	573 609 658	573 612 656	693 757	687 747	691 749	37 650 57 100 44 150	40 600 51 000 32 500	19 250 20 800 17 400	1725	1864	1868
13	**2l**	581 619 671	571 606 655	573 610 665	694 753	685 742	690 748	39 100 60 100 47 300	43 350 53 000 32 300	37 050 35 250 21 950	1746	1903	1900
14	**2m**	579 619 672	571 607 655	573 607 662	690 756	683 745	691 748	34 550 54 400 43 250	39 100 47 550 28 900	37 900 35 250 21 600	1662	1833	2003
15	**2n**	580 618 670	571 607 655	574 611 655	693 760	681 745	692 747	36 400 55 100 42 750	44 600 54 050 32 700	36 400 37 000 22 900	1751	1790	1916
16	**2o**	585 624 677	573 610 658	577 613 665	697 761	684 747	688 749	15 800 27 050 25 500	20 900 27 000 17 950	18 500 23 000 15 900	1678	1773	1778
17	**12**	724	717	724	738	736	738	194 100	163 550	131 850	262	360	262